African Easterly Wave Evolution Pre- and Post-tropical Cyclogenesis

Bryce Tyner[1]

[1]*Department of Marine, Earth and Atmospheric Sciences, North Carolina State University*

May 6, 2010

1. Introduction

There have been a number of studies examining the transformation of African Easterly Waves (AEWs) into tropical cyclones. These studies can be divided into two primary categories: those that emphasize internal processes (eg, Tory et al. 2006a, Hendricks et al. 2004, Dunkerton et al. 2009) and those that emphasize external processes (eg, Shapiro 1977, McBride and Zehr 1981, Pfeffer and Challa 1981) that lead to TC genesis. Kurihara and Kawase (1985) investigated the relative effects of diabatic heating and nonlinear vorticity stretching in this transformation. They concluded the diabatic heating was critical, but development could be enhanced by the additional effect of nonlinearity. With both of these processes acting, the fields of surface vorticity and divergence are coupled such that their interaction leads to contracting and deepening of the surface trough of an AEW. The authors hypothesize this possibly leads to the formation of a distinct vortex. Using a multilevel quasi-geostrophic model, Kwon and Mak (1990) determined AEWs have an inherent thermal structure that makes them unfavorable for TC genesis. This thermal structure stems from a strong thermally indirect circulation so that the vertical motion induced by diabatic heating tends to be destroyed. From the study, the authors determined only waves that can develop a mid-level warm core within a few days are able to develop.

Advocates of internally driven tropical cyclogenesis argue precipitation processes lead to vortex spinup. Some of these advocates argue for the domi-

Corresponding author address: Bryce Tyner, 5148 Jordan Hall NCSU, Raleigh NC 27695
E-mail: bptyner@ncsu.edu

nance of stratiform precipitation processes in TC genesis (eg, Tory et al. 2006a, Tory et al. 2006b, Hendricks et al. 2004). Others argue deep convective precipitation lead to vortex spinup (eg,). The differences between the two internal processes involves whether the initial vortex originates near the surface or in the middle troposphere and is then advected to the surface. While these internal processes are believed to be dominant by these authors, some external forcing can still prevent tropical cyclogenesis even with these strong internal forcings for development, as shown in Tory et al. (2007).

Other studies emphasize external processes as dominant in forcing TC genesis from AEWs. Advocates of this TC genesis mechanism conclude environmentally-induced nonlinear vorticity advection (Shapiro 1977), increased outflow, and angular momentum flux convergence (eg, McBride and Zehr 1981, Pfeffer and Challa 1981, Challa and Pfeffer 1990) lead to TC genesis. These authors conclude that without each of these environmental forcings present, TC genesis is likely to occur.

In association with this controversy over whether internal or external process are more important for TC genesis from AEWs is an even larger conundrum: what happens to the wave when the vortex and eventual tropical cyclone forms? Shapiro (1977) utilizes a parameter that measures the variation of the scale of the wave over its own scale in the Atlantic. With increased meridional wave number, the parameter becomes increasingly small. When this parameter, initially small, becomes large, the system transforms from linear to non-linear dynamics. Using a selected zonal wavelength, he determined that all disturbances which developed from AEWs had a path that intersected a region of this high parameter values. The results suggest a variation in the scale of the wave over its own scale is an important process in the transition from an AEW to a tropical cyclone. Studies in other regions also emphasize this critical role of scale contraction in the process of TC genesis. Sobel and Bretherton (1999) examined disturbances in the tropical western North Pacific, using the NCEP-NCAR reanalysis data set. After applying time filtering, they utilized various techniques including vorticity analyses and ray tracing to examine the evolution of the waves associated with the tropical cyclones. They determined the disturbances propagate as barotropic Rossby waves. In the western North Pacific, wave accumulation occurs due to enhanced convergence. This accumulation allows initially weak disturbances to amplify. After this amplification, they suggest diabatic processes lead to further deepening of the disturbances and eventually strengthening of the tropical cyclone via the WISHE mechanism.

Kuo et al. (2001) utilized a barotropic model to investigate the process

of the transformation of a tropical disturbance into a tropical cyclone. The results of the study suggest the scale contraction of the tropical disturbances could lead to the accumulation of kinetic energy at the longitude where monsoon westerlies and trade wind easterlies meet. The authors envisioned a process in which a wave initially maintains itself via linear processes, before eventually contracting in scale. This scale contraction results in strengthening of the vorticity gradient and nonlinear processes strengthening the disturbance via interactions with the planetary vorticity gradient. Li et al. (2003) utilized QuickStat and TRMM data to examine the source of TC genesis in the western North Pacific. They observe two major processes leading to TC genesis. The first is associated with Rossby wave energy dispersion from existing intense tropical cyclones. The second, similar to the mechanism described by Shapiro (1977) is an energy accumulation mechanism. In both cases, there is a noticeable scale contraction for the wave immediately prior to TC genesis, consistent with the Shapiro (1977) arguements for TC genesis in the Atlantic. The authors were also able to successful model the process of TC genesis for both of these mechanisms.For the second mechanism, the scale contraction for the wave is once again observed. This contraction focuses the PV maximum. Then, resulting convection further enhances the development of the PV disturbance, eventually leading to TC genesis. For the mechanism described, it would appear the contraction of the wave would prevent the wave from continuing to propagate after TC genesis. Fu et al. (2007) utilized this same data set for studying the 2000 and 2001 cases of TC genesis, in addition to utilizing NCEP-NCAR reanalysis data to gain a 3d perspective of the waves. For the same types of pre-storm disturbances described by Li et al. (2003), scale contraction of the disturbances and convergence forcing from large-scale ambient flow were observed to be crucial to TC genesis. In cases with reduced convergence, TC genesis did not occur.

Ferreira and Schubert (1997) examined the breakdown of the ITCZ in a barotropic framework. They utilized a shallow water, barotropic model to examine ITCZ breakdown in the eastern Pacific. They determined the breakdown occurs due to a combination of barotropic and baroclinic instability. The "necessary but insufficient" condition of a reversal in the PV gradient is met in this region due to strong cyclonic PV generated by convection in the ITCZ. If a sufficiently strong perturbation occurs along this PV strip, the strip can break down into several cyclones. These cyclones are attached by a PV tail, which eventually gets wrapped up into the mean circulation. This tail, which was once part of the original PV strip, eventually gets wrapped up into the tropical cyclone's circulation. This process can be seen as analogous to the process by which an AEW forms and transforms into a tropical cyclone. Rather than forming off an ITCZ breakdown, AEWs develop from barotropic

and baroclinic growth along the AEJ. If this analogy is indeed valid, one would then conclude the wave, or PV tail, would be wrapped up in the tropical cyclone's circulation and would thus not be able to continue propagating as its own entity.

The wave is not always wrapped up by the tropical cyclone. NHC storm reports often seem to indicate the wave can continue on and possibly even lead to the formation of another storm. For example, the storm reports for Tropical Storm Franklin and Gert (2005) indicate the same wave was the precursor to both storms. One recent study, Dunkerton et al. (2009), provides some insight into this potential evolution of the wave during TC genesis. In the study, the authors utilized a Lagrangian framework to study TC genesis from AEWs. From their 1998-2001 study based on TRMM and ECMWF data, they develop a "marsupial paradigm" theory for TC genesis from AEWs. The theory emphasizes the need for a closed gye (pouch) where a vortex (embryo) can be protected from dry air intrusion and strengthened by deep convective heating. Eventually, the vortex becomes detached from the wave and acts as its own entity. The wave is thus able to continue to travel on, before eventually dissipating.

a. Motivation

AEWs have been given significant attention by tropical meteorologists. The focus has been on TC genesis processes and the formation of the vortex associated with the tropical cyclones. However, little attention has been given to the fate of the AEW following tropical cyclogenesis. Indeed, understanding the fate of AEWs involved in tropical cyclogenesis is key to understanding the process of tropical cyclogenesis as a whole.

b. Objectives

Motivated by this gap in wave and vortex dynamics, the goals of this study are to answer the following questions:

- What happens to a wave once a tropical cyclone forms?
- Can an AEW survive after tropical cyclogenesis? If so, what are the distinguishing synoptic and mesoscale characteristics that allow the wave to survive versus cases in which the wave does not survive? In the survival cases, is the process analogous to mid-latitude Rossby wave breaking and cut-off low formation?
- In the case where the wave does not survive, what happens to the wave?

Does it dissipate? Does it become absorbed in the circulation of the tropical cyclone? Are the answers to these questions case dependent?

- If there are multiple fates, what is the frequency of occurrence for each fate?

We obtain data of all cases of tropical cyclogenesis in the Atlantic over the time period 2004-2008 using GFS analysis data. We focus on the cases where the source of the initial disturbance for the tropical cyclone was an AEW, and further limit to cases where baroclinic and upper level forcing are negligible. From these cases, categories of the fate of these AEWs after tropical cyclogenesis are developed. Characteristics and a diagnostic for each wave fate category are examined.

c. Data and Methodology

In order to develop the database of case studies, we utilized the GFS analysis data set, available from the National Climatic Data Center (NCDC). This relatively high-resolution, 1 degree grid spacing, data set helps present a relatively accurate depiction of AEWs on synoptic scales during tropical cyclogenesis. The dates and positions of the tropical cyclones was obtained from the National Hurricane Center (NHC) storm archive. Prior to tropical cyclogenesis, the locations of the waves were estimated based on the location of the PV maximum associated with the system. We utilized the McTaggart-Cowan et al. (2008) methodology to narrow down the cases. As explained in their paper, they developed a classification of TC genesis based on the role of lower-level baroclinicity and upper level forcing. They summarized their results into six major categories: nonbaroclinic, low-level baroclinic, transient-trough interaction, trough induced, weak tropical transition (TT), and strong TT. A brief description of each of these categories is described in Table 1. The upper-level forcing is determined by q-vector convergence, using similar methodology as in McTaggart-Cowan et al. (2008). However, rather than computing according to a layer average, we chose to calculate the q-vector convergence at 200 hpa, near the level where typical mid-latitude troughs may be thought to be maximum in amplitude. As in their study, the non-divergent wind was used instead of the quasi-geostrophic wind in computing this q-vector convergence. As noted in their study, the benefit of using this non-divergent wind is the q-vector does not become invalid as the Rossby number becomes large, as would be expected near the tropics. The q-vector was calculated at 200 hpa according to:

$$\vec{Q} = (\frac{\partial u}{\partial x}\frac{\partial \theta}{\partial x} + \frac{\partial v}{\partial x}\frac{\partial \theta}{\partial y})\hat{i} + (\frac{\partial u}{\partial y}\frac{\partial \theta}{\partial x} + \frac{\partial v}{\partial y}\frac{\partial \theta}{\partial y})\hat{j} \quad (1)$$

We defined a high q-vector convergence case as one with a q-vector convergence of at least 2e-15 K/m/s within 10 degrees latitude and longitude for the 36 hours prior to to TC genesis. This q-vector convergence was calculated for all storms from 2004-2008 in the Atlantic. Due to the high subjectivity inherent with the transient-trough interaction category, we decided to include this category in the non-baroclinic cases. Also, due to this subjectivity, we combined the weak and strong tropical transition cases, given the subtle difference in the amount of baroclinicity for these cases. Q-vector convergence was analyzed only for external forcing. Cases in which there was no visible external forcing agent for the q-vector convergence were classified as low q-vector convergence. This was the case for several strong AEWs propagating off the African coast. Likely, these systems already developed many of the dynamics of a tropical cyclone, leading to the q-vector convergence not working as a proper diagnosis for upper level forcing agents. The low-level baroclinicity was measured through a calculation of 1000 hpa-700 hpa layer thickness, as in McTaggart-Cowan et al. (2008). Once again, this layer thickness was calculated within ten degrees of the storm center.

McTaggart-Cowan et al. (2008) determined roughly 40% of TC genesis cases form within the nonbaroclinic environment. They concluded TC genesis occurs much more frequently in this nonbaroclinic environment than in any of the other individual environmental situations. Furthermore, the fate of AEWs is most easily observed in cases with weak environmental forcing. For these reasons, we chose to focus our study on the nonbaroclinic cases with weak baroclinicity and weak upper-level forcing. These nonbaroclinic cases were broken into categories based on the fate of the AEW after TC genesis. Streamlines, PV, and cross-sections were plotted in order to better examine the characteristics of each wave fate classification.

d. Results

1) General Overview

Table 2 examines the breakdown for the 88 tropical cyclones that formed from 2004-2008. Overall, comparing the results of McTaggart-Cowan et al. (2008) with the results from this analysis yields relatively robust results. The percentage of low-level baroclinic TC genesis is almost identical, as well as the percentage of trough induced cases. As expected, the non-baroclnic cases are larger in number than in the McTaggart-Cowan et al. (2008), given the elimination of the transient-trough interaction category. The one major difference in the results of this study versus the previous study is the number of tropi-

cal transition cases, with our study revealing approximately 10% less tropical transition cases. We believe this to be the result of what we define as high q-vector convergence as described above in the methodology section versus the threshold McTaggart-Cowan et al. (2008) utilized. We feel McTaggart-Cowan et al. (2008) may have utilized less strict guidelines for this high q-vector convergence category, leading to more storms in this category.

From this analysis, 59 of the 88 storms were categorized as developing in a non-baroclinic environment. Streamlines at 600 hpa and outgoing long-wave radiation signal (OLR) fields where analyzed in order to determine which of these storms could clearly be tracked back to their origins off the African coast as AEWs. This restraint was placed on the storms in order to isolate traditional Cape Verde AEWs and understand their characteristics well prior to tropical cyclogenesis. Thirty one storms met this categorization and are listed in table 3.

These 31 storms were then analyzed at the 600 hpa, 850 hpa, and 925 hpa levels in order to gain a more 3-dimensional understanding of the wave evolution in the process of TC genesis. The waves were tracked based on a streamline and absolute vorticity analysis. After an analysis of each of these thirty one storms, the storms were placed into 3 major categories, based on the fate of the wave during and after tropical cyclogenesis. These major categories were the wave getting wrapped up in the tropical cyclone's circulation (Type A), the wave splitting from the tropical cyclone (Type B), and a hybrid case where the wave continues propagating with the tropical cyclone (Type C). The category for each storm is listed in table 4.

As seen in the chart, twenty of the thirty one storms fit into the Type A category. The associated AEWs propagate to the west. As TC genesis occurs, and as the storm intensifies, the associated wave becomes no longer visible by the streamline and PV analyses. It can be concluded that the wave either dissolves or became wrapped up in the storm's circulation following TC genesis, in a similar manner as was described by Ferreira and Schubert (1997). In order to better depict the AEW evolution for type A storms, a detailed analysis of one type A storm, Hurricane Dennis (2005) is examined in the following section.

Seven of the thirty one storms analyzed fit into the Type B category. The associated AEWs propagate to the west, similar to the Type A storms. However, at some point in its propagation to the west, the PV associated with the wave appears to split. This split is observed to occur either prior or after tropical cyclogenesis. Lee (2005) interestingly had two splits occur in the PV.

One of these splits occurred prior to tropical cyclogenesis, whereas the other split occurred following tropical cyclogenesis. The evolution of Lee (2005) is presented as a model example of a Type B storm.

Finally, four cases do not appear to fit into either the Type A or B categories. These storms have more of a hybrid evolution. Even following tropical cyclogenesis, the wave continues to be visible and propagates with the tropical cyclone. Gamma (2005) is an example of a Type C storm, and it is analyzed in detail for a comparison with the other categories.

Fig. 1 is a schematic showing the model evolution of each type of wave fate during tropical cyclogenesis. The figure displays the differences in propagation characteristics and structure of the wave during the process of tropical cyclogenesis. All three types of waves display similar initial characteristics, but diverge in time. The Type A waves display a significant tilt in streamlines, the wave becomes wrapped up, and the system begins to propagate with a northward component according to the tropical cyclone's motion. The Type B waves also display a tilt in streamlines, but part of the wave is able to continue propagating to the west, while the other part becomes wrapped up in the tropical cyclone's circulation which propagates with a northward component. Finally, the Type C waves displays a closed circulation, but the system continues to maintain characteristics of the incipient wave, including propagation to the west.

2) Type A Case Study: Hurricane Dennis (2005)

Streamline Analysis Plots of 925 hpa, 850 hpa, and 600 hpa streamlines and vorticity were examined. The signal for AEWs is often strongest near 600 hpa, as has been shown in many previous studies (example Thorncroft and Hodges, 2001). An analysis of streamlines and vorticity at 600 hpa was thus used as a basis for tracking the describing the basic evolution of Dennis. However, most if not all of the results of this 600 hpa vorticity and streamline analysis are robust when compared to the analyses at 850 hpa or 925 hpa. Fig. 2 shows the 600 hpa streamlines and PV at various stages in the development of Dennis. The wave appeared to move off the African coast early on 29th June, as indicated in Fig. 2a. The wave propagated to the west with a phase speed of approximately 55 km/hr. The PV maximum for the wave was relatively weak, with values below 1.5 PVU near the center of the PV maximum. This continued for several days, as shown in Fig. 2b and c. The PV increased significantly at 18z 4 July as shown in Fig. 2d, with PV

values increasing to near 3.5 PVU. The wave appeared to begin contracting as indicated by the streamline analysis. The amplitude increased, while the wavelength began to decrease. At this time, NHC officially declared the system a tropical depression at 12.0°N 60.8°W.

An analysis of the surface winds and minimum sea level pressure indicates the storm then underwent a period of rapid strengthening. According to best track data, the central pressure dropped from 1000 hpa at 00z 6th July to 982 hpa just 24 hours later. Fig. 2e shows the 600 hpa streamlines began to close off around the center of Dennis. The quickly-intensified Dennis likely resulted from a rapidly developing vortex within the wave pocket. It is likely that such a quick disappearance of the open streamlines can be explained by the wave being wrapped up by the quickly-intensified Dennis. As a result, the wave energy was not able to maintain propagation to the west; rather, the wave was ingested by the circulation of the tropical cyclone. An analysis of the deformation field will provide further evidence of this hypothesis.

3) Type B Case Study: Tropical Storm Lee (2005)

Streamline Analysis Once again, an analysis of streamlines and vorticity at 600 hpa was used to summarize the basic evolution of Dennis. The properties of the wave prior to TC genesis appeared quite similar to that of Dennis (2005). The wave moved off the African coast near 25 August, as seen in Fig. 3a. The meridional location of the wave and relative strength are comparable to that for the wave leading to Dennis as it moved off the African coast. The wave appeared to split at around 12z 26 August. As shown in Fig. 3b, there were two local maximas in PV, oriented southwest to northeast with respect to one another. These two local maximas continued to be apparent for the next 48 hours and strengthened somewhat, as shown in Fig. 3c-d. NHC officially declared the system a tropical depression at 12z 28 August. At this time, the vorticity associated with the depression appeared to remained concentrated near the central of the storm, as seen in Fig. 3e. However, by 18z 28 August, the PV began to split once again, as shown in Fig. 3f. One PV center associated with the Lee is indicated by the circle to the northeast. However, to the southwest, another distinct vorticity center began to take shape. The streamlines also displayed a split, with the streamlines near the center of Lee propagating to the northwest according to the storm motion, while the streamlines to the south propagating to the west, according to the parent wave phase speed. By 06z 29 August, the split became even more apparent, as shown in Fig. 3g. A 3 PVU contour was associated with Lee's circulation, with a separate 1.5 PVU PV maximum located to the southwest.

The PV to the southwest continued propagating to the west before dissipating on 31 August. Lee continued propagating to the northwest and eventually to the north, before becoming absorbed within a synoptic scale cold front on 4 September.

Based on an analysis of best track data, Lee did not have a significant period of intensification following tropical cyclogenesis. All strengthening that occurred was much more gradual than that for Dennis. This likely allowed the PV maximum to stretch and eventually break off, both prior and after tropical cyclogenesis. The result was one PV center associated with Lee, with another to the south representing the initial AEW energy. The PV cross sections and deformation analysis that follows illustrate this concept.

PV Cross Sections The splitting of the wave after TC genesis can also be shown via PV cross sections through the wave axis and help provide more of a three dimensional view of the split. Early in the wave's evolution at 06z 26 August, there was a concentrated area of PV extending horizontally only a couple of degrees, with values as high as 2 PVU located near 650 hpa. This is clearly shown in Fig. 4a. While still classified as a wave, the PV field began to split, with two concentrated areas of PV evident by 18z 26 August in Fig. 4b. PV conservation provides evidence that the wave did indeed split, rather than simply the development of a secondary PV maximum. In Fig. 4a, the PV maximum is located within the 312-318K PV regions. In Fig. 4b, the two maximums are also located within this region, tied together by a weaker 1-1.25 PVU region. Based on PV conservation, one would expect PV to be conserved along potential temperature surfaces. This indeed looks likely to be the case within a potential temperature layer, with two weaker maximums in PV for Fig.4b summing together to a value similar to that for the maximum in Fig. 4a.

Following this split, the two portions of the PV continued to propagate to the west. For simplicity purposes, only the portion of the potential vorticity that would become associated with Lee was analyzed in future time steps. At 12z 28 August, as shown in Fig. 4c, this area of PV had a concentrated maximum of PV values of 1.25 PVU or greater extending horizontally over a relatively small area. As noted previously, this is the time in which the system was classified as a tropical depression, according to the National Hurricane Center Best Track data. At 18z 28 August, shown in Fig. 4d, a clear split in the PV occurred within the 600-400 hpa region. A secondary vorticity maximum was located to the southwest of the vorticity center associated with Lee. Over the next day, the vorticity center to the southwest continued to grow, with a PV maximum of near 2 PVU at 06z 29th August. Thus, the

splits prior to and following tropical cyclogenesis can be clearly illustrated in this more three dimensional framework, in addition to the horizontal split illustrated previously.

4) Type C Case Study: Tropical Storm Gamma (2005)

Streamline Analysis The wave that spawned Gamma propagated off the west coast of Africa on 3rd November. Whereas many AEWs that propagate off the coast late in the season do not maintain their strength for extended periods of time, this wave was able to maintain moderate convection through 14 November. The 600 hpa PV field displayed many of the same initial characteristics as for Dennis and Lee, as shown in 5a-c. While centered to the north of central South America, the National Hurricane Center officially declared TC genesis at 00z 14 November. The 600 hpa streamlines and PV at this time are shown in Fig. 5d. The streamlines near the center and to the south of the storm became somewhat closed off at 18z 14 November, as shown in 5e. However, the closed off streamline immediately close to the center of the vortex as surrounded by open streamlines. Similar to the discussion in Dunkerton et al. (2009), the wave and vortex continue propagating together. This evolution continued for a significant amount of time, as shown in 5f. As it continued to propagate to the west, it maintained this wavelike appearance. Eventually, the system once again strengthened as it merged with another area of low pressure near Nicaragua on 17 November, shown in 5g. Thus, the post TC genesis fate of Gamma appeared to have a hybrid evolution, with the tropical cyclone appearing to propagate with the parent wave.

The streamline analysis described correlates well with how the National Hurricane Center best track data classifies the system. Over a period of seven days, the classification from the system transitions from a depression, to a tropical storm, back to a depression, back to a tropical wave, back to a tropical storm, back to a depression, before weakening to a remnant low. Based on this and the streamline analysis, the system did not absorb the wave energy as it encountered tropical cyclogenesis. Rather, the system maintained wavelike characteristics, even as it was classified as a tropical storm.

PV Cross Sections The PV cross section evolution for the Gamma (2005) case provides further evidence of the continued propagation of the wave with the tropical cyclone. The PV max remained near the 600 hpa throughout the storm's evolution, shown in Fig. 6a-d. For typical cases of TC genesis, a vorticity maximum at the surface develops during and remains there after tropical cyclogenesis. The fact the vorticity maximum remains near the 600

hpa after TC genesis provides further evidence for the storm continuing to act as a wave rather than a tropical cyclone. When the storm interacts with the low pressure near Nicaragua at 18z 17th November in Fig. 6e, the vorticity maximum shifts closer to the surface, as the wave begins to get wrapped up in the circulation. In summary, even after being classified as a tropical cyclone by the National Hurricane center, the system continued to maintain properties of a wave rather than a closed vortex for several days. The storm only acted like a vortex following an interaction with a surface low near Nicaragua. This has important implications for the fate of AEWs after tropical cyclogenesis.

e. Dynamical Explanations for Wave Fates

It is important to understand potential sources for each of the three wave fates during tropical cyclogenesis. The sections that follow outline some of the current suggested dynamical causes of the various wave fates.

Intensity Change vs. Type: Type C Evolution For all 31 analyzed tropical cyclones, the rate of intensity change in the 24 and and 48 hours following tropical cyclogenesis were plotted, shown in Fig. 7. The plot clearly shows all of the Type C tropical cyclones display weak rates of intensity change in the period following tropical cyclogenesis. From a conceptual standpoint, for these storms, the developed vortex is relatively weak, even after tropical cyclogenesis. As a result, the weakened vortex is incapable of wrapping the wave up. As a result, the system retains its wavelike features, including its propagation to the west.

For the Type B and Type storms, there is no distinct correlation of rate of intensity change and type. Almost an equal number of storms intensified rapidly for the Type B cases as the Type A cases, as illustrated in the figure. Hence, another explanation must be posed.

Deformation Analysis: Type A vs. Type B Evolution Plots of total deformation were utilized in order to better understand the processes involved in the Type A and Type B wave fates. This deformation was calculated according to:

$$D = \sqrt{Shr^2 + Str^2} \tag{2}$$

where

$$Shr = \frac{\partial u}{\partial x} - \frac{\partial v}{\partial y} \; and \; Str = \frac{\partial v}{\partial x} + \frac{\partial u}{\partial y} \tag{3}$$

The 600 hpa total deformation field was plotted at various times throughout the evolution of Dennis, with the location of the system noted with a black

X. As the wave propagated across the Atlantic, deformation remained quite low for the system. This is shown in Fig. 8a-c. For example, at 06z 3 July in Fig. 8c, there was less than 3e-5 s^{-1} total deformation around the system. As the wave neared TC genesis, however, the deformation significantly increased. At the time of TC genesis at 18z 4 July, there were areas of total deformation to the west and east of the system that were above 8e-5 s^{-1}. This can be seen on Fig. 8b. The high levels of total deformation remained high for the days following TC genesis and also moved to areas south and north of the system, as shown in Fig. 8c. The high total deformation likely promoted the wrap up of the wave within the tropical cyclone. The energy associated with the wave was unable to continue propagating according to the phase speed of the wave.

For Lee (2005), the total deformation also displayed similar characteristics as for Dennis. At 00z 25th August as the system was moving off the African coast, the deformation around the system was relatively week. This is shown in Fig. 9a. At 06z 26 August, an area of high deformation became concentrated within the wave, with values as high as 8e-5 s^{-1}. This is clearly shown in Fig. 9b. Over the next twelve hours, following the occurrence of the split in the area immediately between the two PV maxima, weak deformation re-ensued, as shown in Fig. 9c. This weak deformation continued over the next 24 hours, through the time of tropical cyclogenesis, as evident in Fig. 9c-d. At 00z 29 August, shown in Fig. 9e, the deformation values to the southwest of the PV maximum increased in intensity, up to 8e-5 s^{-1}. As described in the streamline analysis, this is around the time where the wave began to split for the second time. The high deformation values continued for the next twenty four hours.

Based on this analysis, it is suggested that the location of the high deformation was key in determining if the wave split would occur. For both times of wave splitting for Lee, an area of high deformation was observed within the PV maximum. In the following time step, the PV had two localized maxima, rather than one. This differs from Dennis, where the high deformation was located farther away from the PV maximum. The result was the wave became wrapped up within the tropical cyclone circulation and no continued propagation of the wave in that case.

Type B: Example of Wave Breaking? The Type B splitting case demands more attention. Thorncroft et al. (1993) analyzed two idealized baroclinic-wave life-cycles in mid-latitudes. These two life-cycles differ in the sign of the shear in the environment surrounding a mid-latitude trough. In the case of cyclonic vertical shear, the system develops a strong negative tilt, ultimately leading to a wave breaking. The result was a closed cyclone to the north. In the case of anticyclonic vertical shear, the system became positively tilted and also eventually underwent wave breaking. The result was a closed cyclone to

the south of the main trough. Fig. 10 from the paper illustrates these various cases of wave breaking. If inverted, as shown in Fig. 11, the top figure, representing the "anticyclonic" case, appears markedly similar to the schematic shown in Fig. 1b. In particular, the tilt of the wave access in the direction of the wind shear as well as the location of the cut off low resembles each other. The main difference between the Thorncroft et al. (1993) described mechanism and that for the Type B case is a baroclinic shear versus barotropic. The location of tropical cyclogenesis for the case study, Lee (2005), was at a latitude in the subtropics relatively close to the mid-latitude westerlies. Future analysis will examine the horizontal shear pattern for Lee (2005) as well as other Type B cases and compare the shear patterns to the Type A cases.

Type B: Convective Generation of Secondary PV Maximum? The cross sections and streamline plots shown in Figs. 3 and 4 provide some indication that there was a distinct split from the initial PV maximum in the Lee (2005) case study. However, it is worth noting that diabatically generated processes have been found to generate new PV maximas (eg, Brennan and Lackmann 2006). Fig. 12 illustrates this process. Latent heat processes often become dominate during and after tropical cyclogenesis. Hence, it is conceivable latent heat is potential source of the secondary PV developed in the Type B cases. Future studies will conduct a PV budget in order to better isolate the wave breaking mechanism and implications of deformation rather than the convectively generated potential vorticity.

f. Summary and Conclusions

The overarching purpose of this study was to better understand the evolution of the AEW before, during, and after tropical cyclogenesis. In order to provide a basis for comparison, only traditional, nonbaroclinic and non-externally forced AEWs were examined in this study, according to McTaggart-Cowan et al. (2008). Thirty two cases met this criteria. Deformation, streamlines, and PV cross sections were then created for each of these thirty two cases. These cases were then categorized based on these fields and their evolution before, during, and after tropical cyclogenesis. Three major categories emerged from this analysis.

Type A AEWs propagate initially according to their wave phase speed. Immediately prior to tropical cyclogenesis, an area of strong deformation develops outside of the main center of PV. The PV field then becomes concentrated and intensifies as the storm intensifies. The storm then begins to propagate according to the environmental steering current, and the wavelike structure dissipates. The evolution of Dennis (2005) presented in this paper is an ex-

ample of the evolution of a typical Type A case. Based on this study, the majority of waves associated with tropical cyclogenesis follow this evolution.

Much like Type A AEWs, Type B cases propagate according to their wave phase speeds early in their evolution. At some time, an area of significant deformation develops near or within the PV maximum. In the proceeding time steps, the PV associated with the wave begins to split into two distinct maximas. This split can occur either during or after tropical cyclogenesis. In some cases, this split occurs after tropical cyclones. In this case, the tropical cyclone then travels according to the environmental steering current, whereas the wave split off and travels according to its propagation characteristics. The split appears analogous to the "anticyclonic" wave breaking mechanism described in Thorncroft et al. (1993). Future studies will further describe this shearing mechanism for wave splitting. A PV budget will also be conducted in order to isolate this wave breaking mechanism from a convectively generated secondary PV maximum.

Type C AEWs evolves early on like the Type A and B waves, with an area of concentrated PV located near 600 hpa. However, unlike Type A and B cases, following tropical cyclogenesis, the system maintains wavelike characteristics. This includes maintaining its propagation characteristics as well as an open circulation rather than a distinct vortex in the streamline analysis. This evolution provides some evidence of the "marsupial paradigm" described in Dunkerton et al. (2009), with an incipient vortex within a larger AEW.

This study was a preliminary analysis into the fate of AEWs before, during, and after tropical cyclogenesis. It was strictly an observational study, using the GFS analysis data set. Future studies will utilize a modeling framework to better understand the fate of AEWs. From this observational study, it appears the location and strength of the deformation may play a critical role into the fate of the wave following tropical cyclogenesis. Future studies will also seek to examine other critical parameters that may be important to examine in order to better predict the fate of the wave following tropical cyclogenesis. Other years will be examined in addition to 2004-2008 in order to determine the robustness of the preliminary results of this study.

REFERENCES

Brennan, M. J., and G. M. Lackmann, 2006: Observational Diagnosis and Model Forecast Evaluation of Unforecasted Incipient Precipitation during the 24 25 January 2000 East Coast Cyclone. *Monthly Weather Review*, **134**, doi:10.1175/MWR3184.1, 2033–+.

Challa, M., and R. L. Pfeffer, 1990: Formation of Atlantic Hurricanes from Cloud Clusters and Depressions. *Journal of Atmospheric Sciences*, **47**, doi:10.1175/1520-0469(1990)047¡0909:FOAHFC¿2.0.CO;2, 909–928.

Dunkerton, T. J., M. T. Montgomery, and Z. Wang, 2009: Tropical cyclogenesis in a tropical wave critical layer: easterly waves. *Atmospheric Chemistry & Physics*, **9**, 5587–5646.

Ferreira, N. R., and W. H. Schubert, 1997: Barotropic aspects of ITCZ breakdown. *J. Atmos. Sci.*, **54**, 261–285.

Fu, B., T. Li, M. S. Peng, and F. Weng, 2007: Analysis of Tropical Cyclogenesis in the Western North Pacific for 2000 and 2001*. *Weather and Forecasting*, **22**, doi:10.1175/WAF1013.1, 763–+.

Hendricks, E. A., M. T. Montgomery, and C. A. Davis, 2004: The Role of "Vortical" Hot Towers in the Formation of Tropical Cyclone Diana (1984). *Journal of Atmospheric Sciences*, **61**, doi:10.1175/1520-0469(2004)061¡1209:TROVHT¿2.0.CO;2, 1209–1232.

Kuo, H.-C., J.-H. Chen, R. T. Williams, and C.-P. Chang, 2001: Rossby waves in zonally opposing mean flow: Behavior in the Northwest Pacific summer monsoon. *J. Atmos. Sci.*, **58**, 1035–1050.

Kurihara, Y., and M. Kawase, 1985: On the Transformation of a Tropical Easterly Wave into a Tropical Depression: A Simple Numerical Study. *Journal of Atmospheric Sciences*, **42**, doi:10.1175/1520-0469(1985)042¡0068:OTTOAT¿2.0.CO;2, 68–77.

Kwon, H. J., and M. Mak, 1990: A Study of the Structural Transformation of the African Easterly Waves. *J. Atmos. Sci.*, **47**, doi:10.1175/1520-0469(1990)047¡0277:ASOTST¿2.0.CO;2, 277–292.

Li, T., B. Fu, X. Ge, B. Wang, and M. Peng, 2003: Satellite data analysis and numerical simulation of tropical cyclone formation. *Geophys. Res. Let*, **30**, doi:10.1029/2003GL018556, 210000–1.

McBride, J. L., and R. Zehr, 1981: Observational analysis of tropical cyclone formation. Part II: comparison of non-developing versus developing systems. *J. Atmos. Sci.*, **38**, 1132–1151.

McTaggart-Cowan, R., G. D. Deane, L. F. Bosart, C. A. Davis, and T. J. Galarneau, 2008: Climatology of Tropical Cyclogenesis in the North Atlantic (1948 2004). *Monthly Weather Review*, **136**, doi:10.1175/2007MWR2245.1, 1284–+.

Pfeffer, R. L., and M. Challa, 1981: A Numerical Study of the Role of Eddy Fluxes of Momentum in the Development of Atlantic Hurricanes. *Journal of Atmospheric Sciences*, **38**, doi:10.1175/1520-0469(1981)038¡2393:ANSOTR¿2.0.CO;2, 2393–2398.

Shapiro, L. J., 1977: Tropical Storm Formation from Easterly Waves: A Criterion for Development. *Journal of Atmospheric Sciences*, **34**, doi:10.1175/1520-0469(1977)034¡1007:TSFFEW¿2.0.CO;2, 1007–1022.

Sobel, A. H., and C. S. Bretherton, 1999: Development of synoptic-scale disturbances over the summertime tropical North west Pacific. *J. Atmos. Sci.*, **56**, 3106–3127.

Thorncroft, C. D., B. J. Hoskins, and M. E. McIntyre, 1993: Two paradigms of baroclinic-wave life-cycle behaviour. *Quarterly Journal of the Royal Meteorological Society*, **119**, doi:10.1256/smsqj.50902, 17–55.

Tory, K. J., N. E. Davidson, and M. T. Montgomery, 2007: Prediction and Diagnosis of Tropical Cyclone Formation in an NWP System. Part III: Diagnosis of Developing and Nondeveloping Storms. *Journal of Atmospheric Sciences*, **64**, doi:10.1175/JAS4023.1, 3195–+.

Tory, K. J., M. T. Montgomery, and N. E. Davidson, 2006a: Prediction and Diagno-

sis of Tropical Cyclone Formation in an NWP System. Part I: The Critical Role of Vortex Enhancement in Deep Convection. *Journal of Atmospheric Sciences*, **63**, doi:10.1175/JAS3764.1, 3077–3090.

Tory, K. J., M. T. Montgomery, N. E. Davidson, and J. D. Kepert, 2006b: Prediction and Diagnosis of Tropical Cyclone Formation in an NWP System. Part II: A Diagnosis of Tropical Cyclone Chris Formation. *Journal of Atmospheric Sciences*, **63**, doi:10.1175/JAS3765.1, 3091–3113.

Table 1. TC Genesis Categories

TC Genesis Type	Description
Nonbaroclinic	Weak low-level baroclinicity and weak upper level forcing
Low-level baroclinic	Strong low-level baroclinicity and weak upper level forcing
Transient-trough interaction	Trough interaction only immediately prior to TC genesis; variable baroclinicity
Trough induced	Strong upper level forcing and weak baroclinicity
Weak TT	Strong upper level forcing and moderate baroclinicity
Strong TT	Strong upper level forcing and strong baroclinicity

Table 2. TC Genesis Categories

TC Genesis Type	Num. Storms	Perc. of Total
Non-baroclinic	59	68
Low-level baroclinic	9	10
Trough induced	4	5
Weak/Strong TT	16	18

Table 3. Traditional AEWs

Year	Storm Name
2004	Bonnie
	Charley
	Earl
	Frances
	Jeanne
	Karl
	Lisa
2005	Dennis
	Emily
	Franklin
	Gert
	Irene
	TD10
	Lee
	Maria
	Philippe
	Alpha
	Gamma
2006	Chris
	Ernesto
	Florence
	Isaac
2007	Felix
	Ingrid
	Karen
2008	Dolly
	Fay
	Gustav
	Ike
	Nana
	Omar

Table 4. Traditional AEW Categories

Category	Storm Name and Year
Type A	Charley (2004)
	Frances (2004)
	Jeanne (2004)
	Karl (2004)
	Lisa (2004)
	Dennis (2005)
	Emily (2005)
	Gert (2005)
	Irene (2005)
	Philippe (2005)
	Alpha (2005)
	Florence (2006)
	Felix (2007)
	Ingrid (2007)
	Karen (2007)
	Dolly (2008)
	Gustav (2008)
	Ike (2008)
	Nana (2008)
	Omar (2008)
Type B	Franklin (2005)
	Lee (2005)
	Maria (2005)
	Chris (2006)
	Ernesto (2006)
	Isaac (2006)
	Fay (2008)
Type C	Bonnie (2004)
	Earl (2004)
	Gamma (2005)
	TD10 (2005)

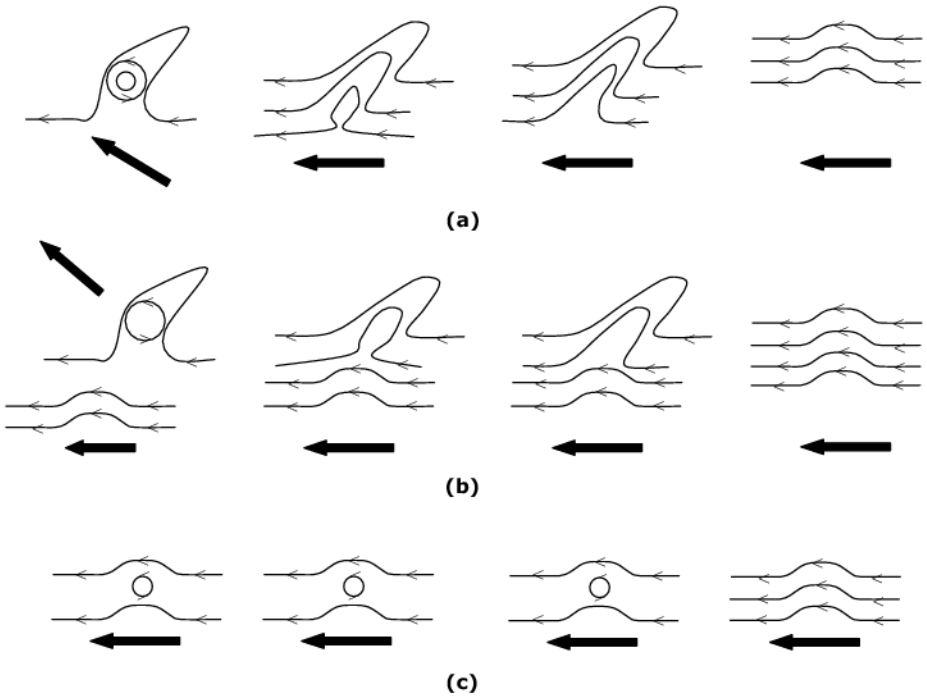

Figure 1. A schematic showing the evolution of the streamlines for a model (a) Type A wrap up case, (b) Type B wave splitting case, and (c) Type C hybrid case. Time in the figures increases to the left.

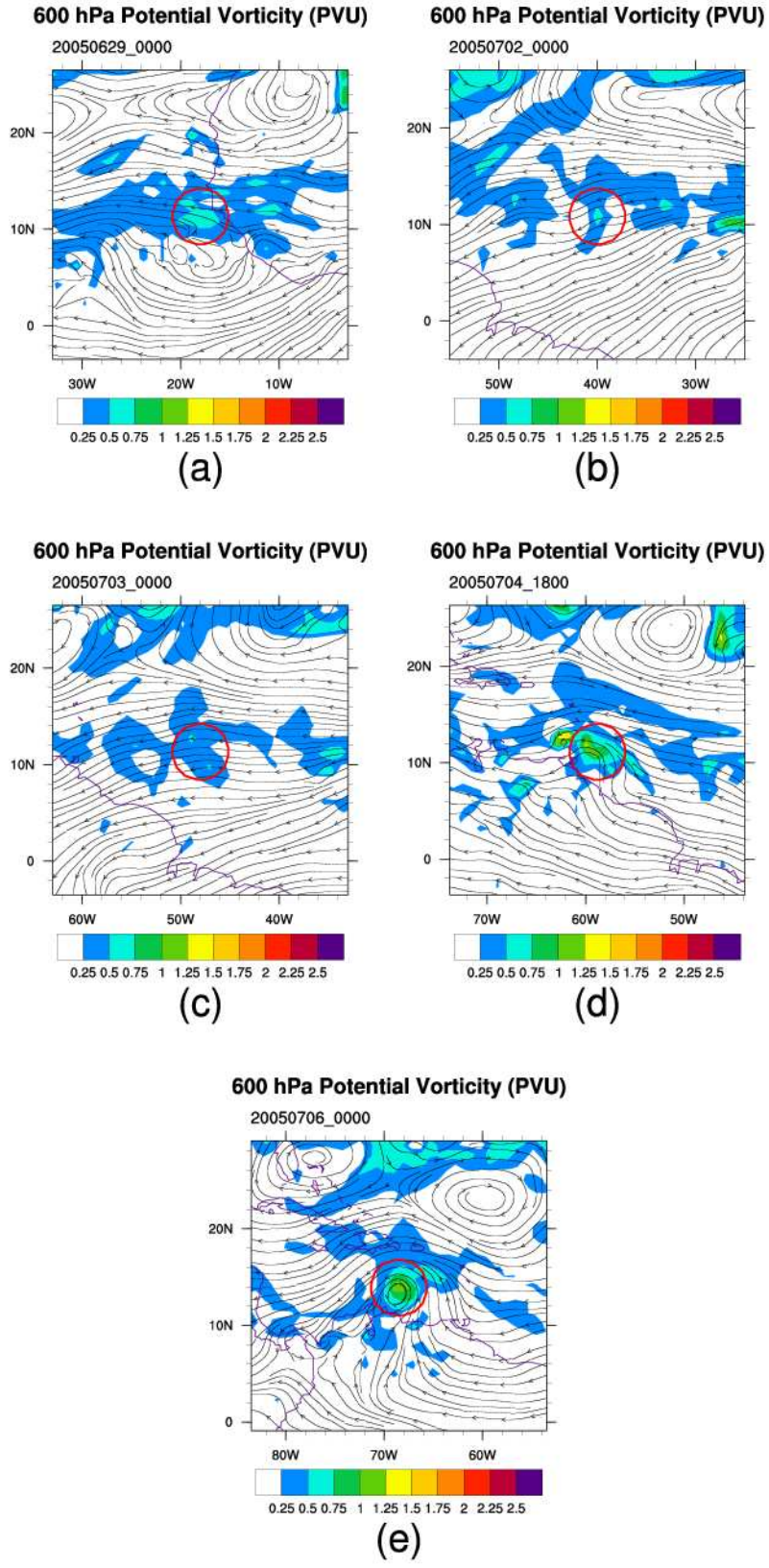

Figure 2. 600 hpa PV and streamlines at (a) 00z 29th June, (b) 00z 2nd July, (c) 00z 3rd July, (d) 18z 4th July, and (e) 00z 6th July. Locations of the system of interest are indicated by a red circle in the figure.

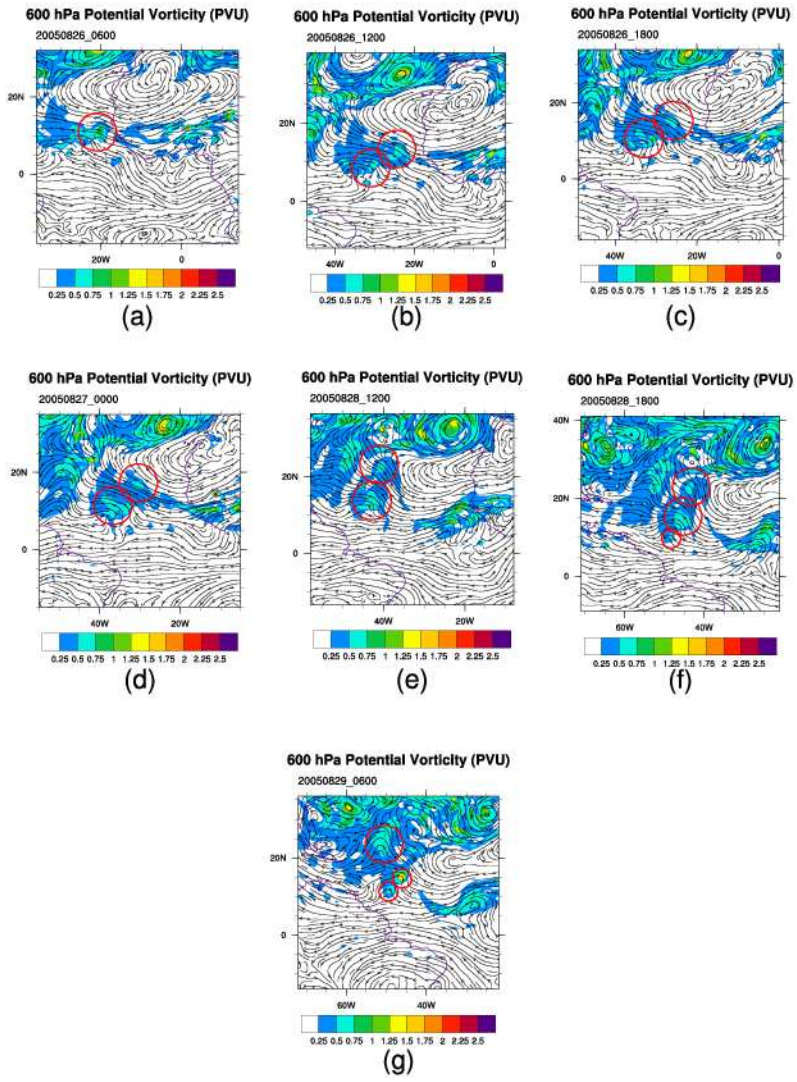

Figure 3. 600 hpa PV and streamlines at (a) 06z 26th August, (b) 12z 26th August, (c) 18z 26th August, (d) 00z 27th August, (e) 12z 28th August, (f) 18z 28th August, and (g) 06z 29th August. Locations of the PV maxes of interest are indicated by red circles in the figure.

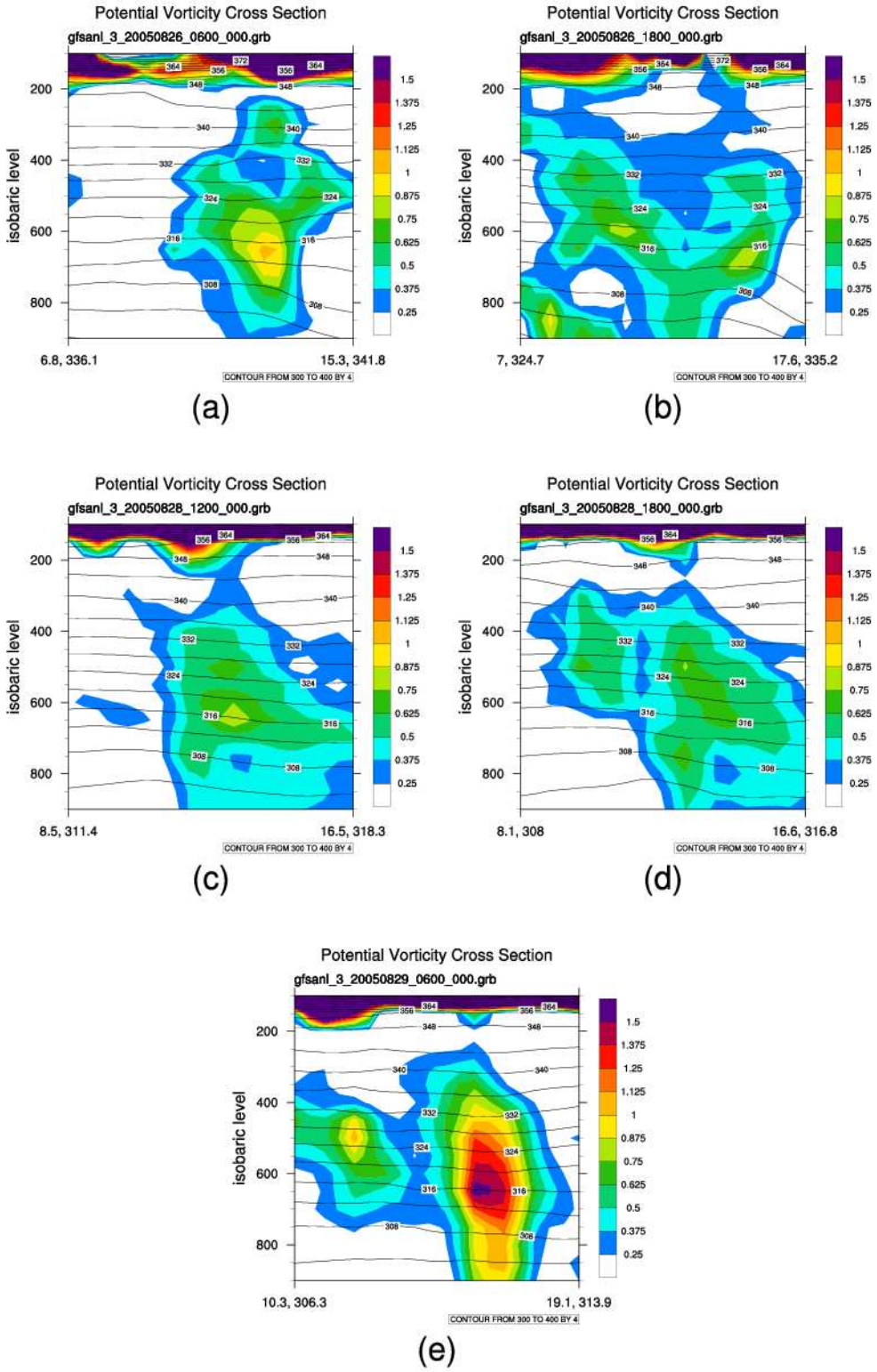

Figure 4. PV cross section through the system of interest and potential temperature contours at (a) 06z 26th August, (b) 18z 26th August, (c) 12z 28th August, (d) 18z 28th August, and (e) 06z 29th August. The lower and upper bounds of the cross section are noted at the bottom of the cross section axes.

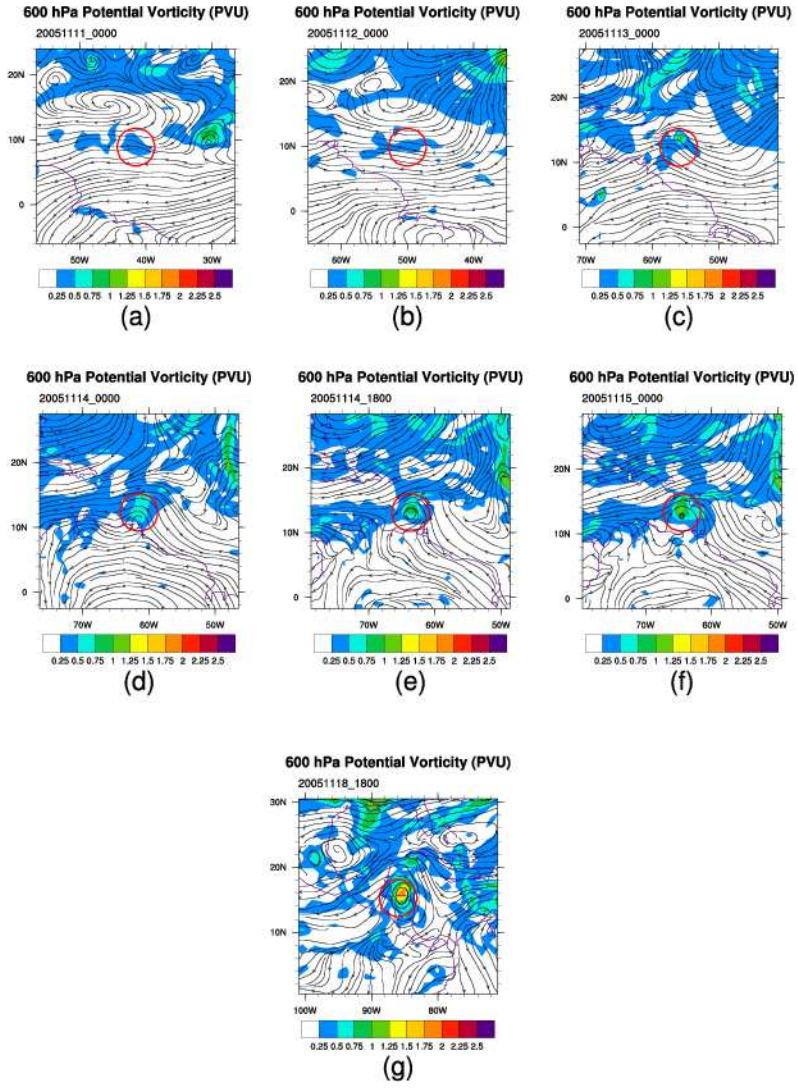

Figure 5. 600 hpa PV and streamlines at (a) 00z 11th November, (b) 00z 12th November, (c) 00z 13th November, (d) 00z 14th November, (e) 18z 14th November, (f) 00z 15th November, and (g) 18z 18th November. Locations of the system of interest are indicated by a red circle in the figure.

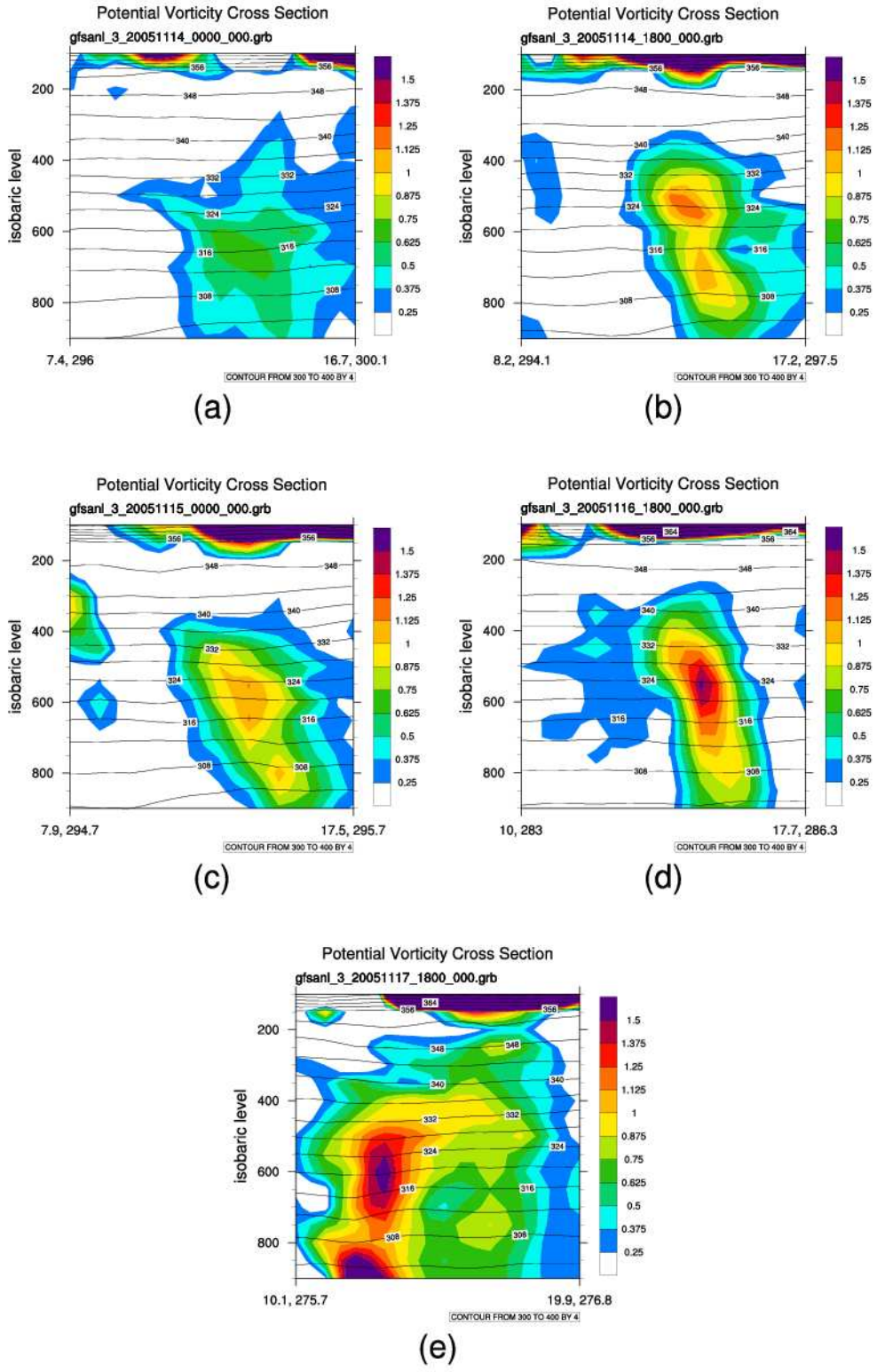

Figure 6. PV cross section through the system of interest and potential temperature contours at (a) 00z 14th November, (b) 18z 14th November, (c) 00z 15th November, (d) 18z 16th November, and (e) 18z 17th November. The lower and upper bounds of the cross section are noted at the bottom of the cross section axes.

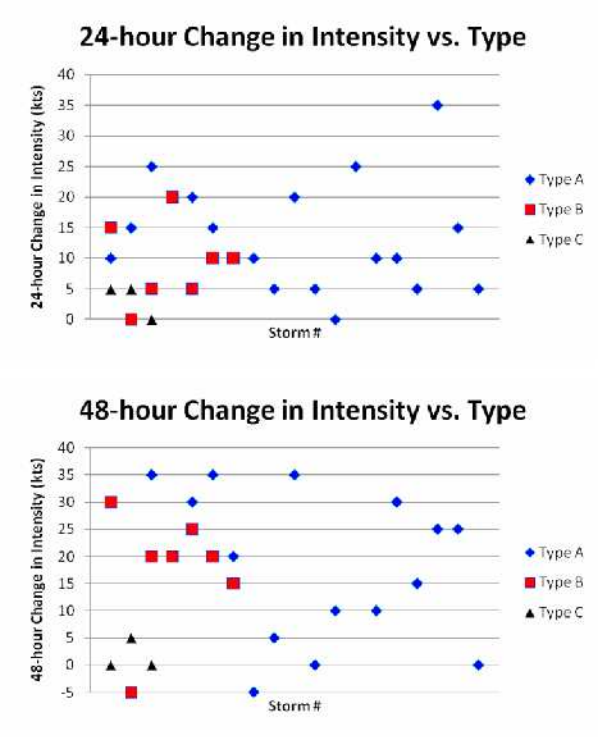

Figure 7. 24 and 48 hour intensity changes following tropical cyclogenesis for all 31 analyzed storms.

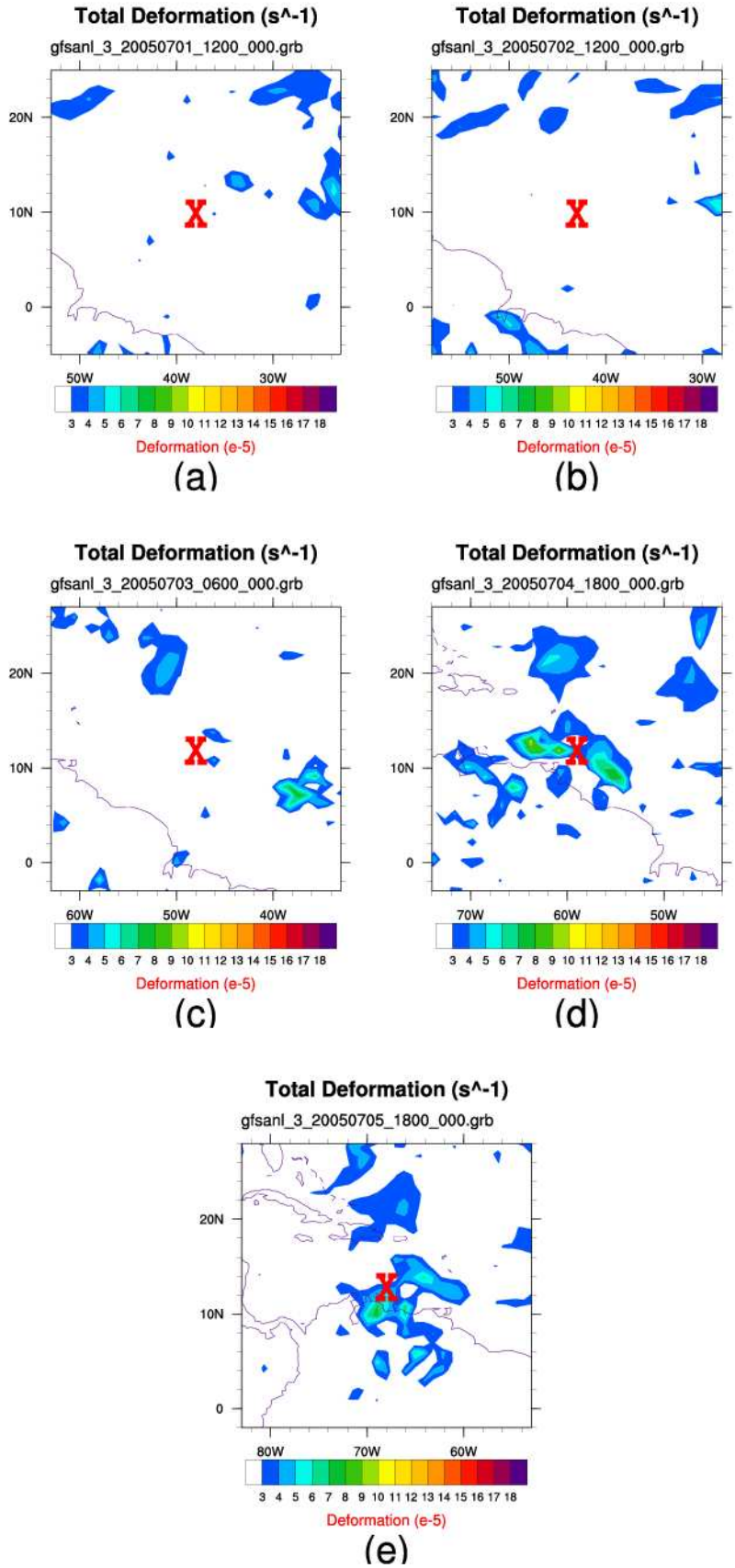

Figure 8. 600 hpa total deformation at (a) 12z 1st July, (b) 12z 2nd July, (c) 06z 3rd July, (d) 18z 4th July, and (e) 18z 5th July. Locations of the system of interest are indicated by a red "X" in the figure.

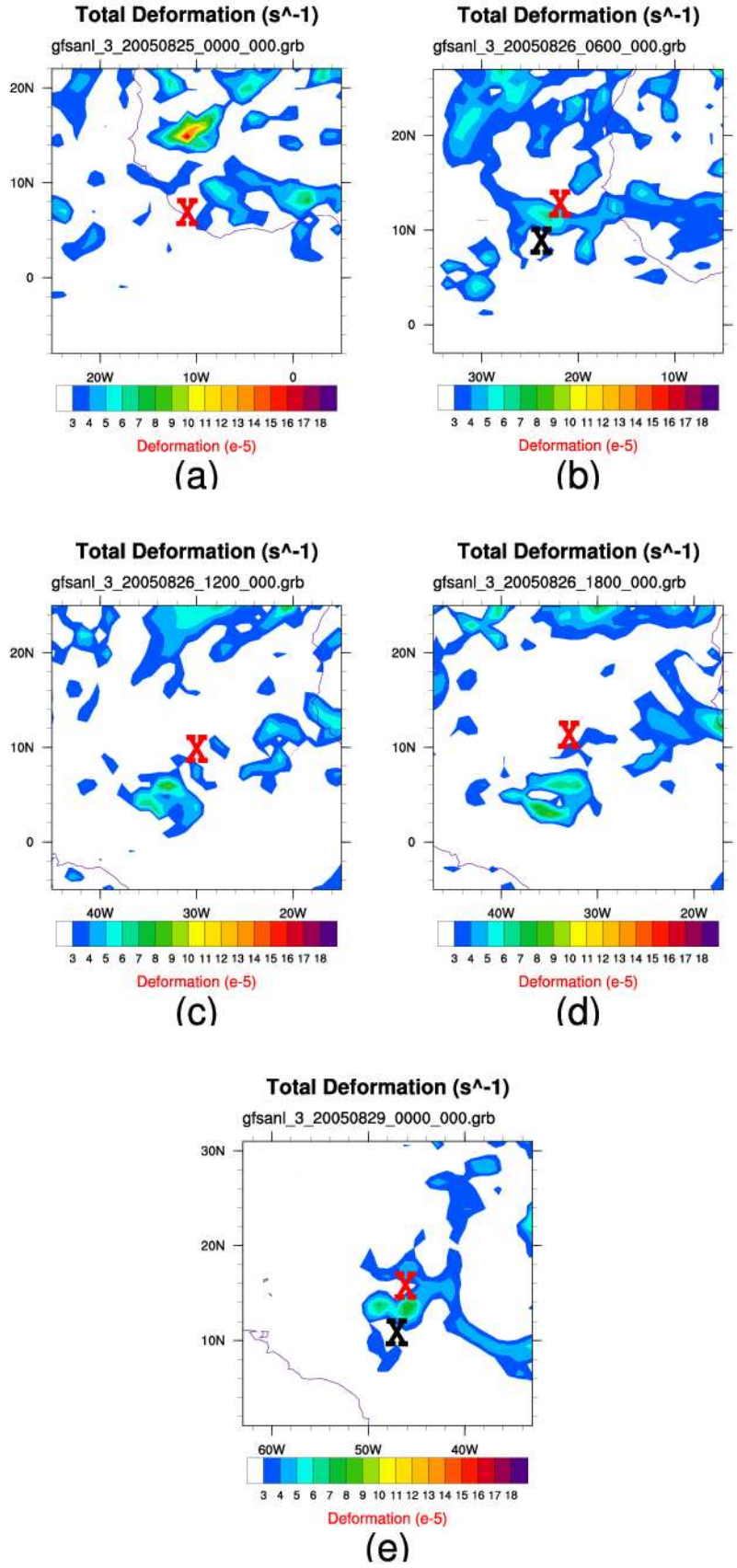

Figure 9. 600 hpa total deformation at (a) 00z 25th August, (b) 06z 26th August, (c) 12z 26th August, and (d) 18z 26th August, and (e) 00z 29th August. Locations of the PV maxima of interest are indicated by "Xs" in the figure.

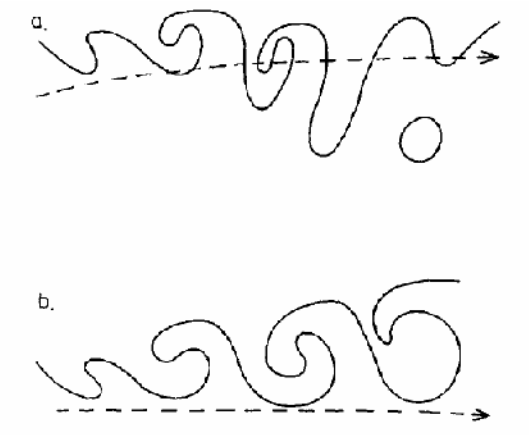

Figure 10. A schematic illustrating "anticyclonic" wave breaking in the mid-latitudes (from Thorncroft et al. 1993).

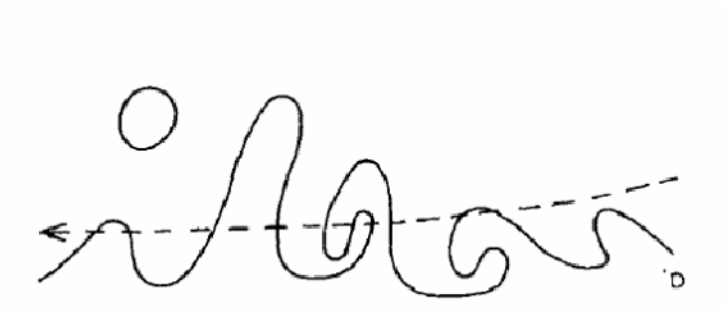

Figure 11. An inverted version of the Thorncroft et al. (1993) "anticyclonic" wave breaking schematic.

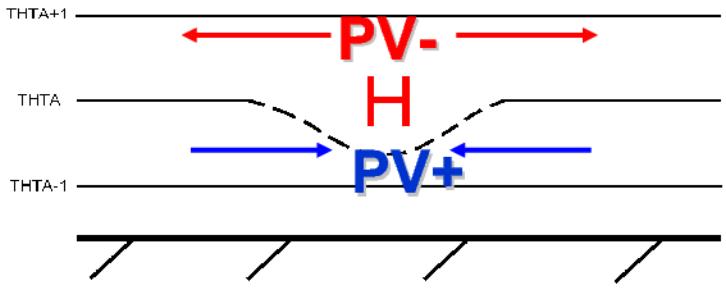

Figure 12. A schematic taken from Brennan (2004), illustrating the process by which latent heat release can lead to a lower tropospheric PV maximum.